Journal of Solid State Chemistry **153,** 34–40 (2000)
doi:10.1006/jssc.2000.8735, available online at http://www.idealibrary.com on IDEAL®

Synthesis and Characterization of the Electron-Doped Single-Layer Manganite $La_{1.2}Sr_{0.8}MnO_{4-\delta}$ and Its Oxidized Phase $La_{1.2}Sr_{0.8}MnO_{4+\delta}$

R. K. Li and C. Greaves[1]

School of Chemistry, The University of Birmingham, Edgbaston, Birmingham B15 2TT, United Kingdom

Received December 27, 1999; in revised form March 27, 2000; accepted April 7, 2000; published online June 27, 2000

The electron-doped single-layer manganite, $La_{1.2}Sr_{0.8}MnO_{3.94}$, has been synthesized under reducing conditions. It has the K_2NiF_4 type structure (space group *I4/mmm*) with a unit cell of $a = 3.82698(2)$ Å and $c = 13.06858(7)$ Å. Magnetic susceptibility study of the as-synthesized sample shows a broad maximum at 110 K, which is attributed to an antiferromagnetic transition. When the sample is treated at 550°C in air, interstitial oxygen is incorporated, resulting in an oxidized phase of composition $La_{1.2}Sr_{0.8}MnO_{4.27}$. The oxidation results in expansion in the *ab* plane ($a = 3.93477(5)$ Å) and a large contraction along the *c* axis ($c = 12.5237(2)$ Å). Although ferromagnetic Mn–Mn interactions are indicated at high temperatures for $La_{1.2}Sr_{0.8}MnO_{4.27}$, they do not lead to any long–range magnetic order at low temperature. Instead, spin glass behavior is observed with a freezing temperature of $T_f = 19.5$ K. © 2000 Academic Press

INTRODUCTION

Layered manganese oxides have been the subject of considerable interest following the reobservation of a large negative magnetoresistance in alkaline-earth-doped La–Mn–O systems (1–3). The coexistence of Mn^{3+} (d^4) and Mn^{4+} (d^3) electronic states in these oxides leads to ferromagnetic (FM) ordering involving a double exchange interaction through Mn^{3+} e_g^1–O_{2p}–Mn^{4+} e_g^0 orbitals, which also triggers the electronic transition from insulator to metal. The interaction strength (reflected by the transition temperature T_c) is lowered when the system dimensionality is reduced from the three-dimensional (3D) infinite layer (La, Sr)MnO_3 ($T_c \approx 350$ K) (4) to the two-dimensional (2D) double-layer compound $(La, Sr)_2Mn_2O_7$ ($T_c = 120$ K) (5). Further decreasing the dimensionality to that of the single-layer $(La, Sr)_2MnO_4$ causes the loss of the FM transition (6). It has now been established that in the single-layer $La_{2-x}Sr_xMnO_4$ system, stoichiometric $LaSrMnO_4$ ($x = 1$) is antiferromagnetic (7), while charge ordering occurs with high hole doping levels, e.g., $x = 1.5$ (8).

The preparation of $LaSrMnO_4$ was initially reported in 1965 (9), and more recently many materials with general composition $La_{2-x}Sr_xMnO_4$ ($x > 1$) have been synthesized under different conditions (10–13). However, to our knowledge, electron-doped materials ($x < 1$) have not been reported. Assuming a tetragonally distorted MnO_6 environment in such materials, the itinerant electrons are within the bands formed by Mn^{2+} $(d_{x^2-y^2})^1$–O_{2p}–Mn^{3+} $(d_{x^2-y^2})^0$, which should also support FM interaction through double exchange via the above $(d_{x^2-y^2})^1$–O_{2p}–$(d_{x^2-y^2})^0$ orbitals. However, the interaction in the electron-doped system should be different from that in the hole-doped La–Mn–O perovskite system, owing to the fundamentally different Coulomb on-site interactions in the two systems. It is interesting, therefore, to investigate whether such an Mn^{2+}–O–Mn^{3+} interaction can also give rise to ferromagnetic order. We have found that electron-doped $(La, Sr)_2MnO_{4-\delta}$ compounds can be synthesized in H_2/N_2 gas mixtures, and in this report we present structural and magnetic results on a typical composition of $La_{1.2}Sr_{0.8}MnO_{4-\delta}$. We also report the formation and properties of the hole-doped oxygen excess phase $La_{1.2}Sr_{0.8}MnO_{4+\delta}$.

EXPERIMENTAL

The conditions for successful synthesis of $La_{1.2}Sr_{0.8}MnO_{4-\delta}$ were first established in thermogravimetric (TG) studies of small samples under reducing conditions. In the final synthesis, a precursor with nominal composition $La_{1.2}Sr_{0.8}MnO_x$ was initially prepared from La_2O_3, $SrCO_3$, and MnO_2. The mixture of starting materials was heated in air at 1100°C for 24 hours with one intermittent grinding. The sintered precursor was powdered and then subjected to heating at 1200°C in a flowing H_2/N_2 gas mixture (10% H_2/90% N_2) for 12 hours; the reduction process was performed twice to achieve a completely

[1] To whom correspondence should be addressed.

0022-4596/00 $35.00

homogeneous black sample. The oxidized phase $La_{1.2}Sr_{0.8}MnO_{4+\delta}$ was prepared by heating the as-synthesized sample in air at 550°C for 6 hours. Powder X-ray diffraction (XRD) patterns were recorded with a Siemens D-5000 diffractometer (monochromated Cu$K\alpha_1$ radiation source, position-sensitive detector, transmission mode). The magnetization of the sample was measured with a Cryogenics S100 SQUID magnetometer. Zero-field-cooled (ZFC) measurements were achieved after the sample was cooled under zero field ($H \approx 0.6$ G) by switching the field on and measuring the magnetization on warming. Field-cooled (FC) measurements were performed by measuring the magnetization during the cooling cycle under an applied field.

RESULTS AND DISCUSSION

The XRD patterns indicated that a single-phase product was formed when the precursor $La_{1.2}Sr_{0.8}MnO_x$ was heated under the H_2/N_2 reducing atmosphere. The pattern was indexed on a body-centered tetragonal unit cell, consistent with a structure related to K_2NiF_4. Structure refinement based on the XRD data (GSAS package (14)); space group $I4/mmm$) confirmed the K_2NiF_4 structure type, and refined unit cell dimensions were $a = 3.82698(2)$ Å and $c = 13.06858(7)$ Å. A 30-point interpolated background and a pseudo-Voigt profile function were used in the refinement. Preferred orientation and anisotropic peak broadening (15) parameters were also refined. With the La : Sr ratio fixed at 0.6 : 0.4 in accordance with that weighed out, variation of the site occupation factors (n) showed that the La/Sr, Mn, and O1 (equatorial, in-plane oxygen) sites are fully occupied, whereas the possibility of a slight deficiency [$n = 0.97(1)$] was indicated at the apical O2 site. However, since correlation effects precluded simultaneous refinement of the O2 temperature factor and site occupancy, the temperature factor for this site was constrained to what was considered a realistic value ($U_{iso} \times 100 = 0.8$ Å^2). The fitted XRD profile is shown in Fig. 1, and the refined parameters are given in Table 1. Given the constraints discussed above, the deviation of the O2 occupancy from unity may be insignificant, and the sample composition is certainly close to $La_{1.2}Sr_{0.8}MnO_4$. The precise oxygen content of this precursor is not, however, of fundamental importance to the subsequent discussion, which will therefore be based on the refined O2 occupation and the corresponding chemical formula $La_{1.2}Sr_{0.8}MnO_{3.94(2)}$. Irrespective of the oxygen content, it is clear that the compound is genuinely electron doped: the Mn oxidation state is +2.68 for the composition $La_{1.2}Sr_{0.8}MnO_{3.94(2)}$ and +2.80 for $La_{1.2}Sr_{0.8}MnO_4$.

Refinement of the oxidized phase suggested a closely related structure. Since the weight change from TG analysis during oxidation of the sample corresponds to an uptake of 0.33 mole of oxygen per mole of $La_{1.2}Sr_{0.8}MnO_{3.94}$ (to give $La_{1.2}Sr_{0.8}MnO_{4.27}$), an additional oxygen position (O3) was introduced into the refinement, at the interstitial sites between the two La/Sr layers. Due to high correlation

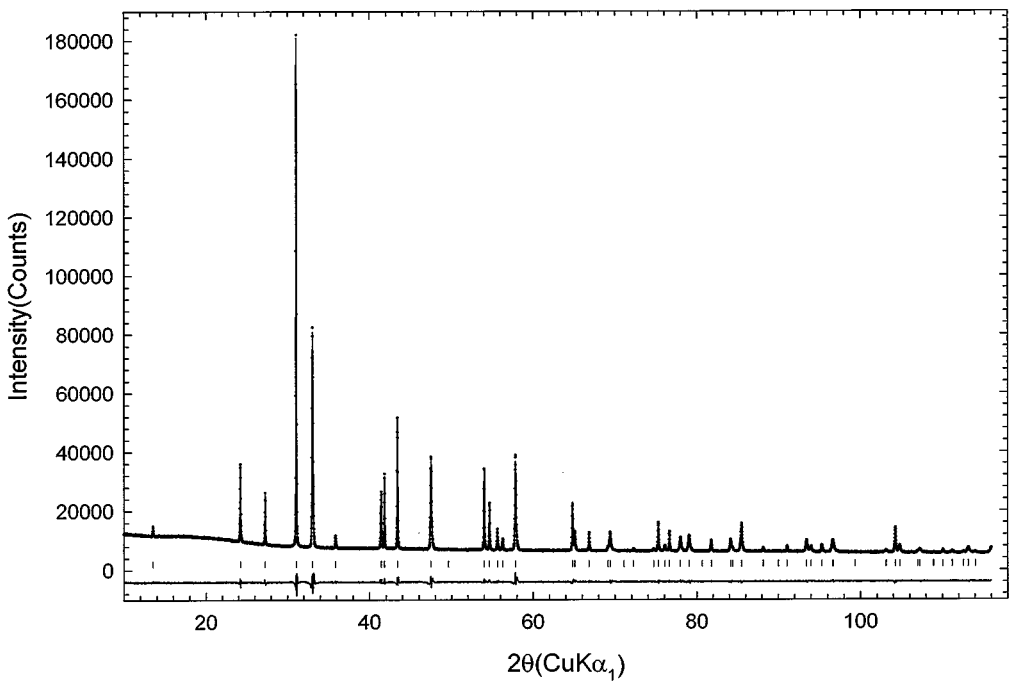

FIG. 1. Observed (dots), calculated (line), and difference XRD patterns of $La_{1.2}Sr_{0.8}MnO_{3.94}$ (the vertical bars beneath the observed pattern represent the diffraction peak positions).

TABLE 1
Refined Atomic Parameters of $La_{1.2}Sr_{0.8}MnO_{3.94}$[a] and Its Oxidized Phase $La_{1.2}Sr_{0.8}MnO_{4.27}$[b]

	$La_{1.2}Sr_{0.8}MnO_{3.94}$					$La_{1.2}Sr_{0.8}MnO_{4.27}$				
Atoms	*x*	*y*	*z*	$U \times 100/Å^2$	*n*	*x*	*y*	*z*	$U \times 100/Å^2$	*n*
La/Sr	0.5	0.5	0.14270(4)	0.56(2)	0.6/0.4	0.5	0.5	0.14491(7)	1.93(4)	0.6/0.4
Mn	0	0	0	0.65(5)	1	0	0	0	0.99(8)	1
O1	0.5	0	0	0.8(1)	1	0.5	0	0	2.3(2)	1
O2	0	0	0.1738(3)	0.8[c]	0.969(5)	0	0	0.1555(8)	6.6(2)	1
O3	—	—	—	—	0	0.0	0.5	0.25	1.8(17)	0.135[c]

Note. $U_{iso} = B_{iso}/8\pi^2$. The numbers in parentheses are estimated standard deviations from the least-squares refinement.
[a] Space group *I*4/*mmm*, $a = 3.82698(2)$ Å, $c = 13.06858(7)$ Å, $R_{wp} = 2.26\%$, $R_p = 1.46\%$, $\chi^2 = 4.28$.
[b] Space group *I*4/*mmm*, $a = 3.93477(5)$ Å, $c = 12.5237(2)$ Å, $R_{wp} = 2.40\%$, $R_p = 1.89\%$, $\chi^2 = 1.18$.
[c] fixed.

effects between atomic coordinates, temperature factors, and occupation factors, O2 was assumed fully occupied and the O3 occupancy was constrained to 13.5%, in accordance with TG analysis. Satisfactory agreement indices ($R_{wp} =$ 2.40% and $\chi^2 = 1.18$, Fig. 2) were achieved by refining the anisotropic broadening of the diffraction peaks as in the reduced phase. It should be noted that no evidence for occupancy of this interstitial site was found for the reduced phase.

The refined atomic parameters are listed in Table 1 and selected bond distances in Table 2. The refinement is consistent with TG analysis and suggests that oxidation at 550°C forms a sample with chemical formula $La_{1.2}Sr_{0.8}MnO_{4.27}$. The temperature factor for O2 is rather high [$U_{iso} \times 100 = 6.6$ Å^2 ($B_{iso} = 5.2$ Å^2)], but is consistent with the partial occupation of the O3 site (13.5% occupied), which will distort the neighboring O2 sites. The high La/Sr temperature factor can also be attributed to local disorder caused by partial occupancy of O3, since this site is the closest coordinated anion to the La/Sr site (Table 2). Oxidation of $La_{1.2}Sr_{0.8}MnO_{3.94}$ to $La_{1.2}Sr_{0.8}MnO_{4.27}$ results in an increase in unit cell volume from 191.40(1) to 193.90(1) Å^3 which relates to an expansion of *a* (from 3.8270 Å to 3.9348 Å, + 2.8%) and contraction of *c* (from 13.0686 Å to

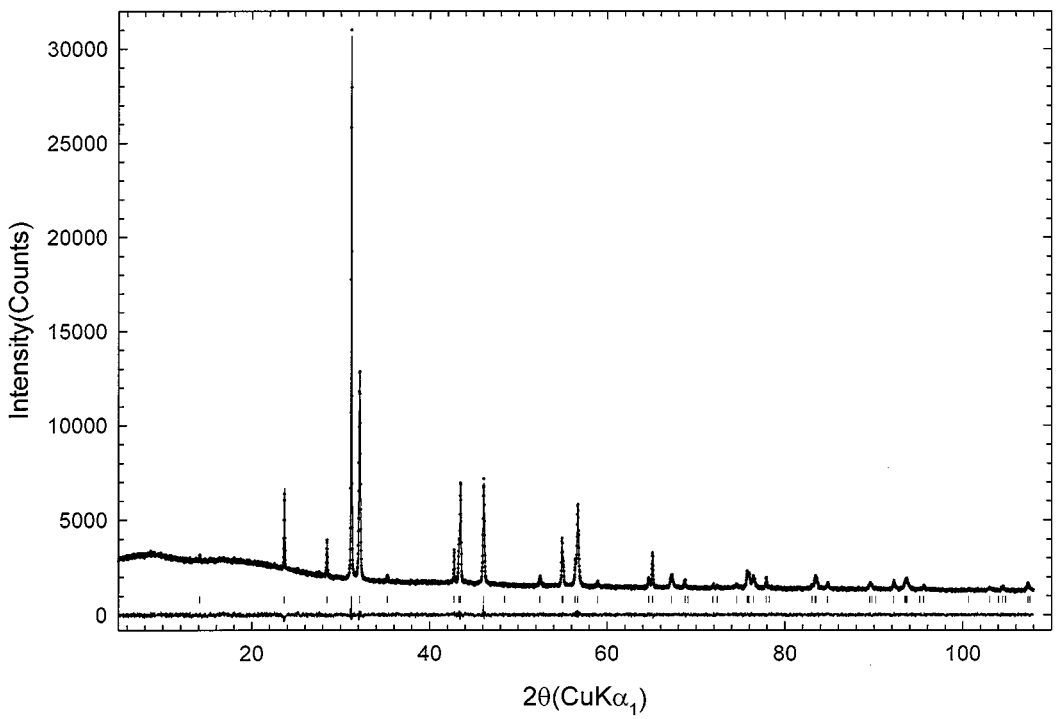

FIG. 2. Observed (dots), calculated (line), and difference XRD patterns of $La_{1.2}Sr_{0.8}MnO_{4.27}$.

TABLE 2
Bond Lengths (Å) in $La_{1.2}Sr_{0.8}MnO_{3.94}$ and $La_{1.2}Sr_{0.8}MnO_{4.27}$

Bonds	$La_{1.2}Sr_{0.8}MnO_{3.94}$	$La_{1.2}Sr_{0.8}MnO_{4.27}$
La/Sr–O1x4	2.6719(3)	2.6766(6)
La/Sr–O2x4	2.7366(5)	2.7856(4)
La/Sr–O2x1	2.397(4)	2.497(9)
La/Sr–O3x4	—	2.3670(5)
Mn–O1x4	1.9135(1)	1.9674(1)
Mn–O2x2	2.272(4)	1.950(9)

12.5238 Å, −4.2%). This observation can explain the discrepancy between two reports on the unit cell parameters of a related compound, $LaSrMnO_4$. The values reported by Blasse ($a = 3.88$ Å, $c = 12.5$ Å) (9) are suggestive of an oxidized phase, while those obtained by Benabad *et al.* (10) ($a = 3.804$ Å, $c = 13.10$ Å) are consistent with an oxygen-deficient material. It is clear that the in-plane Mn–O1 bond length is increased after oxidation, but the apical Mn–O2 bond length is dramatically reduced, from 2.27 Å to a value (1.95 Å) which is even shorter than the Mn–O1 in-plane bond (1.97 Å). This slight compression in the apical Mn–O2 bond will clearly affect the *d*-orbital energies of the Mn cations in the MnO_2 plane. It is well known that Mn^{3+} (d^4) is subject to Jahn–Teller distortions, whereas both Mn^{2+} (d^5, high spin) and Mn^{4+} (d^3) are not. However, the substantial reduction in *c* after oxidation cannot simply reflect the decrease in concentration of the Mn^{3+} ion in the compound, since the reduced phase contains a level of Mn^{3+} concentration (68% Mn^{3+}; 32% Mn^{2+}) similar to that of the oxidized phase (66% Mn^{3+}; 34% Mn^{4+}). Moreover, the Jahn–Teller distortion normally leads to elongated apical bonds in the K_2NiF_4 type structure (16), whereas in the oxidized phase the reverse is suggested. The structure changes could be consistent with disproportionation of Mn^{3+} to Mn^{2+} and Mn^{4+} in the oxidized phase, since both Mn^{2+} and Mn^{4+} ions prefer undistorted octahedral sites. However, no clear stabilization is apparent for such a charge segregation, and in the many studies reported on maganese oxides with Mn oxidation state between 3 and 4, we are unaware of any strong evidence for the disproportionation of Mn^{3+}. Although we cannot rule out such an electronic description, we prefer to retain the normal model involving Mn^{3+} and Mn^{4+}, and the following discussion of the results obtained is based on this assumption. The contraction in *c* associated with oxidation is probably caused by the need to accommodate the interstitial oxygen ions. As a result, in the oxidized phase the $d_{x^2-y^2}$ orbital of Mn^{3+} is stabilized relative to the dz^2 orbital, in contrast to the case for normal Jahn–Teller distortions. This interesting observation means that for both the reduced and oxidized phases in the $La_{1.2}Sr_{0.8}MnO_{4\pm\delta}$ system, the charge carriers should be located within the $d_{x^2-y^2}$–$O2p_{x,y}$–$d_{x^2-y^2}$ orbitals in the MnO_2 plane.

The magnetic susceptibility of the reduced phase is shown in Fig. 3. A broad maximum is observed at 110 K, which is

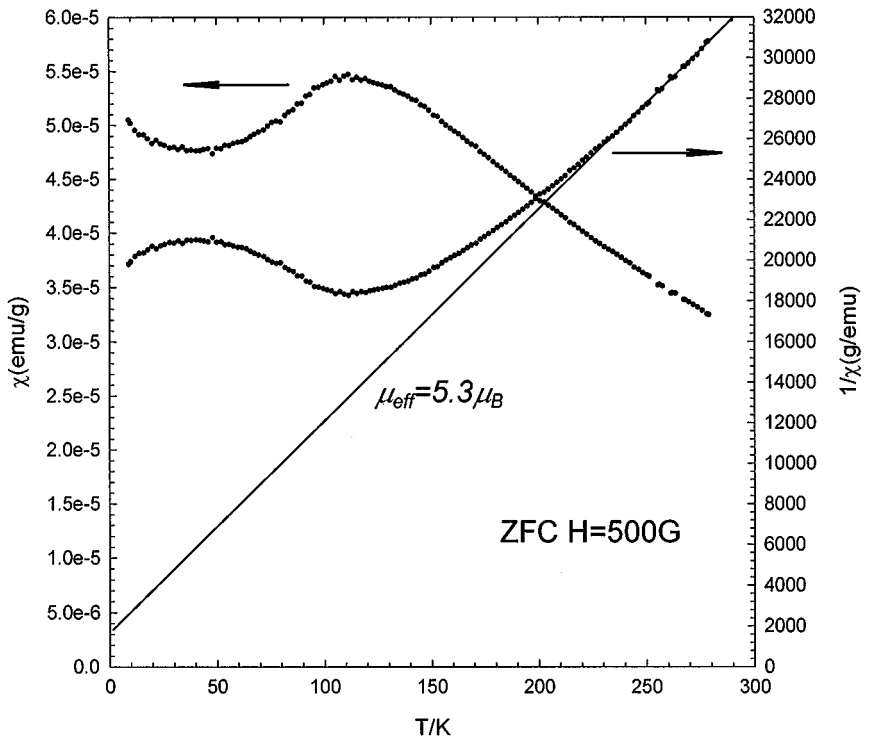

FIG. 3. Magnetic susceptibility of $La_{1.2}Sr_{0.8}MnO_{3.94}$.

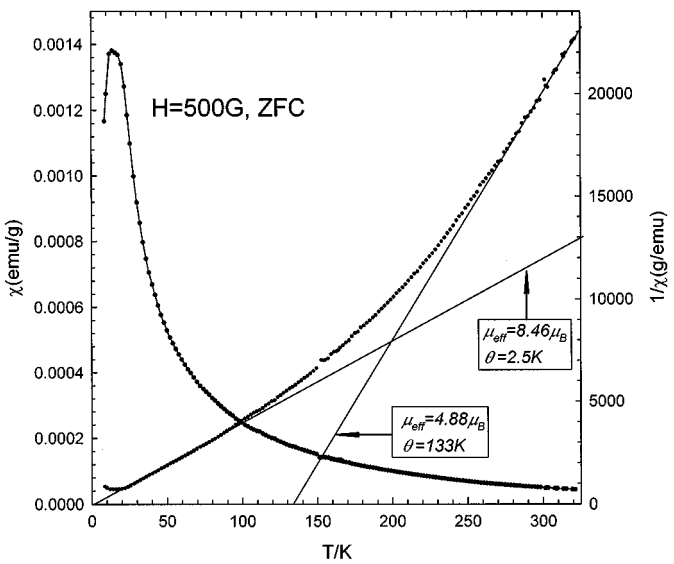

FIG. 4. Magnetic susceptibility (zero field cooled) of $La_{1.2}Sr_{0.8}MnO_{4.27}$.

an indication of antiferromagnetic (AFM) ordering in this 2D system. From the electronic states of the Mn^{2+}/Mn^{3+} ions in the compound, as mentioned above, it can be predicted (17) that ferromagnetic (FM) interactions should occur *via* Mn^{2+} $(d_{x^2-y^2})^1$–O2*p*–Mn^{3+} $(d_{x^2-y^2})^0$ superexchange and double-exchange interactions. The discrepancy between this prediction and our observation of AFM order may be rationalized by the following situations. First, in the Mn–O plane charge ordering of Mn^{2+}/Mn^{3+} into clusters or stripes may occur as observed in related hole-doped La_2CuO_4 and La_2NiO_4 compounds (18, 19). In such a case, clustering to produce a predominance of nearest-neighbor interactions of the type Mn^{2+}–O–Mn^{2+} and Mn^{3+}–O–Mn^{3+} will occur, both of which give AFM interactions. Alternatively, there could indeed be FM interaction between the Mn^{2+}/Mn^{3+} ions within the MnO_2 layer, but AFM order may occur between the layers at $T_N = 110$ K. The first mechanism is supported by the observation of the broadening of the XRD diffraction peaks with in-plane indices, e.g., (*hk*0) reflections are broader than (00*l*) reflections. Incorporation of this anisotropic broadening into the Rietveld refinement was essential to achieve a satisfactory fit and the broadening is consistent with local order within the MnO_2 plane, which has also been observed in $La_{0.5}Sr_{1.5}MnO_4$ (13).

Ferromagnetic interactions are observed in the high-temperature range for the oxidized phase $La_{1.2}Sr_{0.8}$

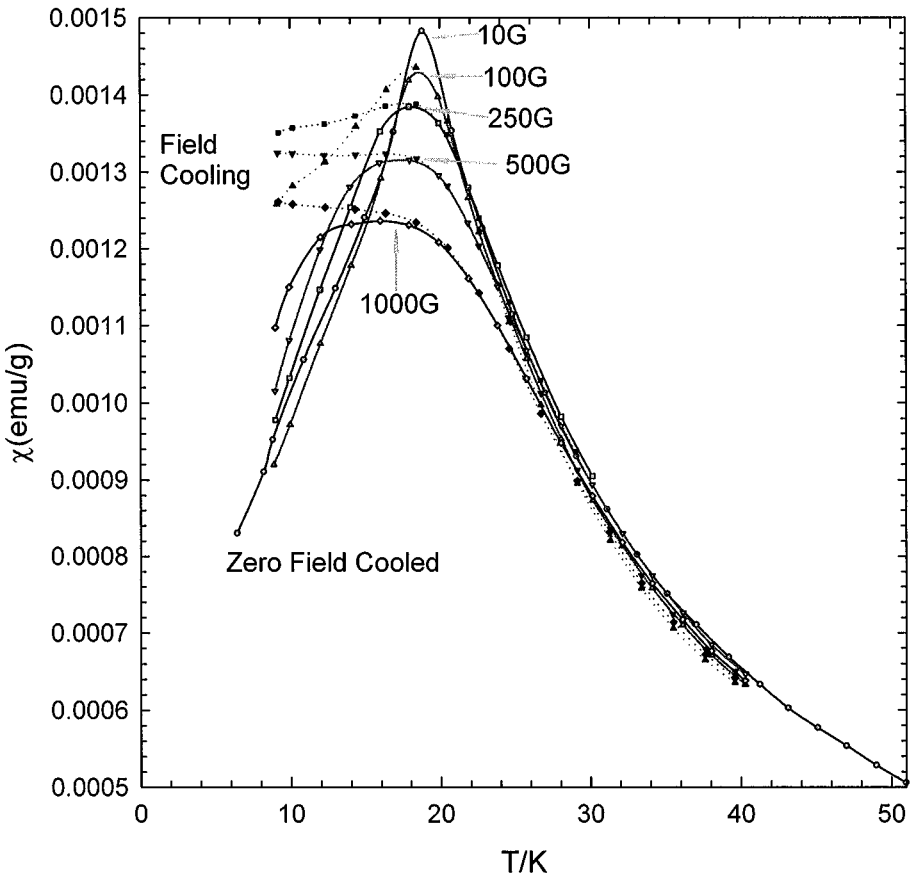

FIG. 5. Magnetic susceptibilities (ZFC and FC) of $La_{1.2}Sr_{0.8}MnO_{4.27}$ at low temperature under different fields.

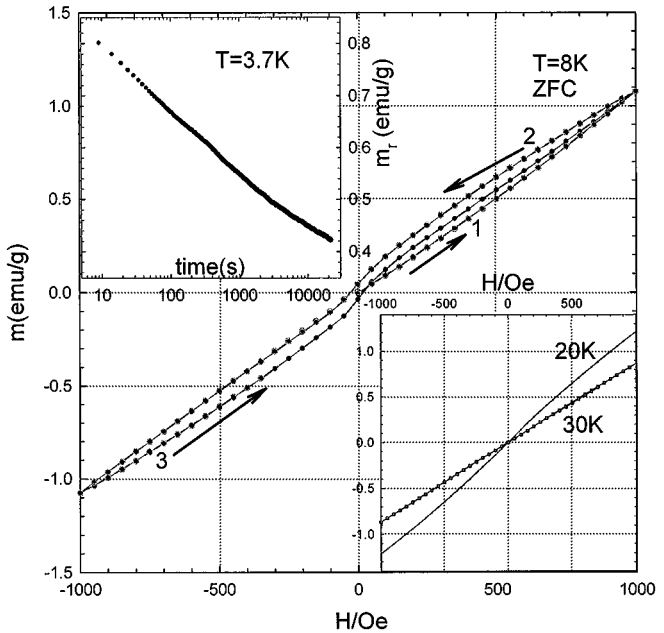

FIG. 6. Hysteresis loop of $La_{1.2}Sr_{0.8}MnO_{4.27}$ at 8 K. The numbers and arrows indicate the sequence of the field sweeps. The right bottom corner inset shows the field dependence of magnetization at 20 K and 30 K without any hysteresis. The left top inset shows the time dependence of the remnant magnetization (cooled in $H = 4$ Tesla field from 50 K).

$MnO_{4.27}$ (Fig. 4). Above 250 K, application of the Curie–Weiss law ($\chi = C/(T-\theta)$) provides a positive θ value ($\theta = 133$ K), indicative of FM interactions, and an effective moment on the Mn ion of $\mu_{eff} = 4.88\ \mu_B$, which is very close to the theoretical spin-only value of Mn^{3+} (4.9 μ_B). When the temperature is lowered, however, the effective moment increases whereas θ decreases. In the low-temperature range (20–100 K), the Curie–Weiss law yields $\mu_{eff} = 8.46\ \mu_B$ and $\theta = 2.5$ K. The enhanced magnetic moment suggests the presence of FM clusters of about four Mn ions. Although spins within the clusters are aligned parallel, the resultant moments on individual clusters are randomly distributed. In addition, a cusp is seen at low temperature in the zero-field-cooled (ZFC) magnetic susceptibility. Below the temperature of the cusp, T_f, deviation between ZFC and field-cooled (FC) susceptibility was observed. The position and sharpness of the cusp are field dependent (Fig. 5), e.g., $T_f = 19.5$ K for $H = 10$ G and $T_f = 16$ K for $H = 1000$ G; the FC susceptibility is flattened in sufficiently large fields (> 250 G). All aspects of the above behavior are characteristic of spin glass (SG) behavior (20): for example, growth of the Mn effective moment was observed in an Ag–Mn alloy (21) and the flattening of the FC susceptibility is consistent with that observed in (Fe, Mn)TiO_3 (22). It is also normal that $1/\chi$ versus T plots display a decrease in gradient on cooling (such as that shown in Fig. 4) for spin glasses with FM interactions, whereas AFM spin glasses show an increased gradient (23). A very narrow hysteresis loop (ZFC, Fig. 6) was observed below the freezing temperature, T_f, with small coercive field $H_c < 50$ G and a small remnant magnetization (M_r). The remnant magnetization (FC) of $La_{1.2}Sr_{0.8}MnO_{4.27}$ decreases with time with a roughly ln t dependence (Fig. 6, top left inset), which is again in accordance with SG behavior (23).

To show such SG behavior, the system requires the presence of inherent AFM interactions to compete with the FM exchange, which is dominant within the FM clusters. Such an interaction could originate from the local ordering of the Mn^{3+} and Mn^{4+} ions. Recalling that in $La_{1.2}Sr_{0.8}MnO_{4.27}$ the MnO_6 octahedra are compressed, which stabilizes the $d_{x^2-y^2}$ orbital, we see that in the MnO_2 plane the same FM $(d_{x^2-y^2})^1$–O2p–$(d_{x^2-y^2})^0$ interaction occurs as in the reduced phase, which is consistent with the positive Curie–Weiss constant (θ) observed. However, when the charge carriers (holes) are localized in a fashion to provide nearest-neighbor Mn^{3+}–O–Mn^{3+} and Mn^{4+}–O–Mn^{4+} arrangements, superexchange will give the necessary AFM interactions. For example, FM clusters comprising mixed Mn^{3+}–Mn^{4+} could be linked *via* AFM Mn^{3+}–Mn^{3+} or Mn^{4+}–Mn^{4+} pairs. We therefore believe it is the competition between double-exchange (Mn^{3+}–O–Mn^{4+}) and superexchange (Mn^{3+}–O–Mn^{3+}, Mn^{4+}–O–Mn^{4+}) interactions which results in the observed SG behavior of $La_{1.2}Sr_{0.8}MnO_{4.27}$. It is worth noting that SG behavior was also reported for the hole-doped $La_{1-x}Sr_{1+x}MnO_4$ system with $0.2 < x < 0.6$, although detailed discussion was not given (12). The valence state of Mn in $La_{1.2}Sr_{0.8}MnO_{4.27}$ corresponds to that for $x = 0.34$ in $La_{1-x}Sr_{1+x}MnO_4$, which obviously lies in the SG region. As for the structure data, it is possible to rationalize the magnetic data by assuming the presence of Mn^{2+} and Mn^{4+} ions, rather than Mn^{3+} and Mn^{4+} ions. However, for the reasons indicated above, we have elected to base our interpretation of the results, and discussion, on the latter electronic description.

CONCLUSIONS

The electron-doped single-layer manganite $La_{1.2}Sr_{0.8}MnO_{3.94}$ has been synthesized in an H_2/N_2 gas flow. It can be oxidized to $La_{1.2}Sr_{0.8}MnO_{4.27}$ by heating in air at 550°C, the incorporated oxygen occupying the interstitial sites in the K_2NiF_4 type lattice. It is found that the in-plane Mn–O1 bond is elongated while the apical Mn–O2 bond is very much contracted during oxidation. The reduced phase shows a 2D AFM transition with a broad maximum at 110 K, whereas the oxidized phase shows FM interactions at high temperature but enters an SG state below $T_f = 19.5$ K.

ACKNOWLEDGMENTS

We thank EPSRC for financial support.

REFERENCES

1. R. M. Kusters, J. Singleton, D. A. Keen, R. Mcgreevy, and W. Hayes, *Physica B* **155,** 362 (1989).
2. R. V. Helmolt, J. Wekker, B. Holzapfel, L. Shultz, and K. Samwer, *Phys. Rev. Lett*. **71,** 2331 (1993).
3. S. Jin, T. H. Tiefel, M. McCormack, R. A. Fastnacht, R. Ramesh, and L. H. Chen, *Science* **264,** 413 (1994).
4. G. H. Jonker and J. H. van Santen, *Physica* **16,** 337 (1950).
5. Y. Moritomo, A. Asamizu, H. Kuwahara and Y. Tokura, *Nature* **380,** 141 (1996).
6. R. A. Mohan Ram, P. Ganguly, and C. N. R. Rao, *J. Solid State Chem.* **70,** 82 (1987).
7. S. Kawano, N. Achiwa, N. Kamegashira, and M. Aoki, *J. Phys. C* **8,** 829 (1988).
8. B. J. Sternlieb, J. P. Hill, U. C. Wildgruber, G. M. Luke, B. Nachumi, Y. Moritomo, and Y. Tokura, *Phys. Rev. Lett*. **76,** 2169 (1996).
9. G. Blasse, *J. Inorg. Nucl. Chem.* **27,** 2683 (1965).
10. A. Benabad, A. Daoudi, R. Salmon, and G. le Flem, *J. Solid State Chem.* **22,** 121 (1977).
11. J. C. Boulox, J. L. Soubeyroux, A. Daoudi, and G. le Flem, *Mater. Res. Bull.* **16,** 855 (1981).
12. Y. Morimoto, Y. Tomioka, A. Asamitsu, Y. Tokura, and Y. Matsui, *Phys. Rev. B* **51,** 3297 (1995).
13. W. Bao, C. H. Chen, S. A. Carter, and S. -W. Cheong, *Solid State Commun.* **98,** 55 (1996).
14. A. C. Larson and R. B. Von Dreele, "General Structure Analysis System," Los Alamos National Labotatory, Los Alamos, NM, 1994.
15. P. Stephens, *J. Appl. Crystallogr.* **32,** 281 (1999).
16. P. Ganguly and C. N. R. Rao, *J. Solid State Chem.* **53,** 193 (1984).
17. J. B. Goodenough, *Phys. Rev.* **100,** 564 (1955).
18. J. M. Tranquada, B. J. Sternlieb, J. D. Axe, Y. Nakamura, and S. Uchida, *Nature* **375,** 561 (1995).
19. J. M. Tranquada, D. J. Buttrey, and V. Sachan, *Phys. Rev.* **B 54,** 12318 (1996).
20. J. A. Mydosh, "Spin Glasses: an Experimental Introduction," Taylor & Francis, London, 1993.
21. R. V. Chamberlin, M. Hardiman, L. A. Turkevich, and R. Orbach, *Phys. Rev. B* **25,** 6720 (1982).
22. A. Ito, H. Aruga, E. Torikai, M. Kikuchi, Y. Syono, and H. Takei, *Phys. Rev. Lett*. **57,** 483 (1986).
23. K. V. Rao, M. Fähnle, E. Figueroa, O. Beckman, and L. Hedman, *Phys. Rev. B* **27,** 3104 (1983).
24. P. Nordblad, P. Svedlindh, L. Lundgren, and L. Sandlund, *Phys. Rev. B* **33,** 645 (1986)